THE JOURNAL OF PHYSICAL CHEMISTRY B

ARTICLE

pubs.acs.org/JPCB

A Criterion for Anomalous Melting in Systems with Isotropic Interactions

Gianpietro Malescio*,† and Franz Saija‡,§

†Dipartimento di Fisica, Università degli Studi di Messina, Viale F. Stagno d'Alcontres 31, 98166 Messina, Italy

‡CNR-IPCF, Viale F. Stagno d'Alcontres 37, 98158 Messina, Italy

ABSTRACT: The relationship between anomalous (re-entrant) melting and the features of the repulsive part of the intermolecular potential is studied in one-component systems with radially symmetric interactions. By making use of the Lennard-Jones−Devonshire cell model, we derive a single-phase criterion for the occurrence of a temperature maximum in the melting line. The criterion is tested against numerical simulation results for a number of isotropic interaction models.

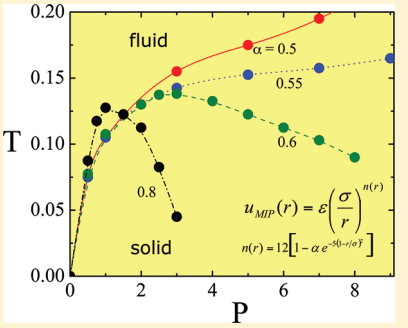

I. INTRODUCTION

In prototypical (i.e., argon-like) simple fluids, the solid−liquid coexistence line runs monotonically to high temperatures with increasing pressures. In contrast with this "standard" behavior, melting is termed "anomalous" when the melting line shows a temperature maximum followed by a re-entrant region where melting occurs upon compression at constant temperature.[1] A remarkable consequence of this behavior is the coexistence of the solid with a denser liquid, a well-known example being provided by ice and liquid water. Usually, re-entrant melting is associated with other anomalous features such as polymorphism in the liquid and solid phases, as well as a number of thermodynamic, dynamic, and structural (TDS) anomalies that include the density anomaly (a decrease in density upon cooling), the diffusion anomaly (an increase of diffusivity upon pressurizing), and the structural anomaly (a decrease of structural order for increasing pressure).[2,3]

The most well-known class of systems displaying anomalous behaviors is that of the network-forming fluids, i.e., fluids characterized by orientation-specific intermolecular bonds, such as water, silicon, phosphorus, and silica.[2,4−8] Due to such intermolecular bonds, there is more empty space between molecules than in simple liquids such as argon. Pressurizing distorts the bond structure and increases the number of particles in the first coordination sphere, thus causing a density increase. This originates two local fluid structures with different density competing with each other, which leads to re-entrant melting (see section II). Another relevant example of anomalous melting is provided by the behavior of many elements under extremely high pressures such as, e.g., Rb, Cs, K, Ba, Sr, Ca, Li, Na, N_2, H, and C.[1,9−17] Pressure-induced modifications of the electronic structure may cause a sudden drop in the effective radius of the atom (as in Cs where an "orbital collapse" occurs), or a gradual shrinking of the atomic radius as can be expected for lighter and smaller chemical elements. These modifications of the atomic effective length scale are reflected in one or more regions of re-entrant melting. *Ab-initio* computer simulations support the experimental evidence of anomalous melting at high pressures and temperatures in hydrogen,[18−20] nitrogen,[21] light alkali metals,[22,23] and carbon.[24]

The quest for understanding the origins of anomalous behaviors has given impulse to the study of simple models that are nevertheless able to display anomalous behaviors. Such systems represent generic models for pure metals, metallic mixtures, electrolytes, and colloidal systems. As far as unbounded interactions are concerned, it has been found that unusual behaviors may arise in one-component systems of spherical particles where the diverging repulsive core is "softened" through the addition of a finite repulsion at intermediate distances, so as to generate two distinct length scales: a "hard" one, related to the inner core, and a "soft" one, associated with the soft, penetrable, component of the repulsion.[3,25−46] Due to this feature, such core-softened (CS) fluids are characterized by two competing, expanded and compact, local arrangements of particles. This property, although arising from simple isotropic interactions, effectively mimics the behavior of the much more complex network-forming fluids, where loose and compact local structures arise from the continuous formation and disruption of the dynamic network originated by orientational bonds. Recently, the two-scale picture as a requisite for anomalous behaviors has been challenged by a

Special Issue: H. Eugene Stanley Festschrift

Received: April 28, 2011
Revised: July 18, 2011
Published: September 07, 2011

study showing that even a weak softening of the repulsive interparticle interaction, though not able to yield two distinct length scales, may nevertheless give origin to anomalous behaviors.[47]

In this paper, we present a study that aims at assessing the extent to which interparticle repulsion has to be softened in order to yield anomalous behaviors. In particular, we investigate, by calculating the Lindemann ratio through the use of the Lennard-Jones cell theory, the conditions for the occurrence of a temperature maximum in the melting line.

II. ANOMALOUS MELTING

The relationship among the different kinds of anomalous behavior is a debated issue. In particular, it is still unclear whether anomalous behaviors all imply each other. Water, the most well-known substance displaying anomalous features, appears to be characterized by a full spectrum of anomalous behaviors, including re-entrant melting as well as a wealth of TDS anomalies (often called *water-like*), although a direct observation of a liquid−liquid phase transition (LLPT), suggested by a number of indirect evidence, is not possible since the liquid−liquid critical point lays in an experimentally unaccessible metastable region.[48−63] The possibility that liquid polymorphism may occur disjointed from TDS anomalies was recently raised by the experimental study of triphenyl phosphite, where in association with the LLPT the heat capacity shows no anomalous behavior, and a density increase is expected upon cooling.[64,65] As it concerns CS model systems, re-entrant melting is usually associated with TDS anomalies,[3] and, in the presence of a suitable attractive component, to LLPT.[37,40] However, in some cases, the region of TDS anomalies is located in the pressure−temperature phase-diagram inside the region where the solid phase is the most stable, and thus it is inaccessible with equilibrium simulations.[43,66]

In general, anomalous melting and LLPT appear to be closely related, as can be highlighted, for example, through the use of a simple "two-state" model liquid that contains low and high-density species.[67] The proportion of high-density domains increases with increasing pressure, so that the liquid density eventually exceeds that of the underlying solid, and the melting line thus passes through a temperature maximum followed by an anomalous region of negative dT/dP slope. Since the chemical composition of low and high-density domains is the same, a "regular solution" mixing model can be applied. In such solution models, at low temperature a liquid−liquid critical point appears, below which a LLPT occurs between liquid polymorphs that have the same chemical composition, but different densities and entropies. The existence of such density/entropy-driven polymorphic liquid−liquid transition is announced by the occurrence of a melting curve maximum (followed by a negative melting slope), as well as by polyamorphic behavior in amorphous solids.

In the following, we focus on anomalous melting as a fundamental phase feature for the general occurrence of water-like anomalous behaviors. Consequently, we restrict our analysis to systems with unbounded purely repulsive interactions. Our aim is to derive a criterion that can be used to guess, from the functional form of the intermolecular potential, the occurrence of anomalous melting in systems with isotropic interactions.

III. THEORY

The starting point of our analysis is the well-known Lindemann melting law.[68] According to this law, a solid melts when the mean-square amplitude of the vibrations of atoms about their equilibrium position becomes larger than a certain fraction of the lattice spacing. To evaluate the Lindemann fraction L

$$L = \frac{1}{d}\left\langle \frac{1}{N}\sum_{i=1}^{N}(\Delta R_i)^2 \right\rangle^{1/2} \tag{1}$$

where d is the nearest neighbor distance, N is the number of particles, and the brackets denote the average over the dynamic trajectories of the particles, we adopt the Lennard-Jones−Devonshire cell model.[69,70] In this model, each atom is confined within its cell and moves in the potential field $U(r)$, generated by its neighbors. This potential field is obtained by summing the pair potentials $u(r)$ over all the stationary neighbors of the central atom and taking a spherical average.

To calculate the Lindemann fraction, we adopt the harmonic approximation:

$$U(r) = U(r_0) + \frac{1}{2}K(r - r_0)^2 \tag{2}$$

where $(r - r_0)$ is the displacement of the atom from its static equilibrium position r_0 and K, following ref 71, is the reduced force constant:

$$K = \frac{1}{3}\left(\frac{\nu}{c}\right)^{2/3}\sum_i z_i\left[\frac{2\phi'(r_i)}{r_i} + \phi''\right] \tag{3}$$

Here the pair potential has been written as $u(r) = \varepsilon\phi(r/\sigma)$ (ε and σ being the energy and length units), $\phi'(r) = d\phi(r)/dr$ and $\phi''(r) = d^2\phi(r)/dr^2$, $\nu = (1/\sigma^3)V/N$ is the reduced volume, z_i is the number of ith neighbors in the crystal lattice of the solid considered, $r_i = c_i(\nu/c)^{1/3}$, and c_i and c are constant depending on the geometry of the crystal lattice. The values of r_i to be used in performing the summation in eq 3 depend on the lattice that, for the chosen interaction model, corresponds to the most stable solid phase.

If $K/t \ll 1$, where t is the reduced temperature $t = k_B T/\varepsilon$, the Lindemann fraction can be written as $L \approx (3t/K)^{1/2}$, i.e., $t \approx (1/3)L^2K$.[71] Thus, a melting curve maximum will occur if K has a maximum as a function of volume. Accordingly, for the volume ν_{max} corresponding to the maximum melting temperature, the condition $\partial K/\partial\nu_{|\nu=\nu_{max}} = 0$ should hold.

From eq 3 it follows that

$$\partial K/\partial\nu = \sum_i b_i r_i^{-2} F(r_i) \tag{4}$$

where

$$b_i = \frac{1}{3}c_i z_i/c^{1/3} \tag{5}$$

and

$$F(r) = 2\phi'(r) + 4r\phi''(r) + r^2\phi'''(r) \tag{6}$$

In order that the summation in eq 4 may vanish, it should include both positive and negative terms (unless all terms are zero). Since the coefficients b_i are positive, as well as r_i^2, if $F(r)$ is strictly positive (or negative), the condition $\partial K/\partial\nu = 0$ will never be satisfied, independently of the lattice considered (on which the specific values of r_i depend), and, consequently, the melting line will have no maximum. Thus, in order that anomalous melting may be possible, $F(r)$ should change sign over its definition domain. This provides a simple criterion that expresses, in terms of the interaction potential and its derivatives, a *necessary*

condition (from which the name n-criterion used in the following originates) for the occurrence of anomalous melting. This criterion can be applied to potentials that are differentiable with their first and second derivative. Moreover, since cell theories are based on the assumption that each atom is confined within its cell, the interparticle potential $u(r)$ should possess a steep repulsive core, and, in order that the average potential field $U(r)$ may be calculated, $u(r)$ should decay for large r faster than $1/r^2$. It can be easily verified that for inverse-power potentials with $n > 1$, $F(r)$ is everywhere negative and thus the n-criterion is not satisfied, as expected since these potentials are characterized by a monotonously increasing melting line.

IV. NUMERICAL SIMULATION

To estimate the melting line, we perform Monte Carlo (MC) simulations in the isothermal−isobaric NPT ensemble, i.e., at constant temperature T, pressure P, and number N of particles, using the standard Metropolis algorithm with periodic boundary conditions and nearest image convention. The simulations have been carried out for a number of particles ranging from $N = 686$ for a body-centered cubic (bcc) crystal and $N = 864$ for a face-centered cubic (fcc) crystal (we also checked that finite-size effects are negligible). We generate a sequence of simulation runs along an isobar, using as the starting configuration a low-temperature perfect crystal whose density is set equal to its $T = 0$ value at that pressure. The series of runs is continued until a sudden density/energy change is found. Since the density of a solid phase ordinarily varies very little with increasing temperature along an isobar, a sudden density change indicates a mechanic instability of the solid in favor of the fluid, and thus signals the approximate location of melting as is also confirmed by the rounding off of the peaks of the radial distribution function $g(r)$.

This procedure allows one to locate the upper stability threshold of the solid when heated isobarically, i.e., the superheated solid spinodal (SSS). By calculating the SSS, we estimate the topology of the melting line, and thus we are able to locate the threshold between the regimes of standard and anomalous melting. The reliability of this approach has been tested by verifying that the solid−fluid coexistence lines obtained through "exact" free-energy calculations (see ref 44 for technical details), although laying at lower temperatures, preserve the topology exhibited by the SSS, and thus the estimates of the standard-anomalous melting threshold provided by the two approaches agree with each other.

In order to study thermodynamics and structural anomalies, we performed a chain of NPT runs both along isotherms and isobars starting from a sufficiently dilute-fluid state or from a high temperature configuration, respectively. To evaluate the diffusion coefficient, we have performed classical molecular dynamics (MD) simulations in the canonical NVT ensemble, i.e., at constant temperature T, volume V, and number N of particles, using a system composed by $N = 864$ particles. All MD runs have been carried out starting from a sufficiently dilute-fluid state for each temperature T and density ρ. Diffusivity was computed using the Einstein relation.

Systems with softened interparticle repulsion are characterized by a rich solid polymorphism, i.e., by the existence of many different stable crystal phases at low temperature.[72] When investigating the melting behavior, solid polymorphism represents a complication since the number of crystals that are potentially relevant for the system at hand is enormous. A common simplification consists in restricting the calculation of chemical potential to just those phases that are found stable or nearly stable at zero temperature. In the range of pressures here considered, the stable phases for the systems investigated are the fcc and the bcc crystals.[73] This result is used for calculating the SSS and the fluid−solid coexistence points.

V. RESULTS AND DISCUSSION

To devise an elucidative test of the above derived criterion, we consider several families of intermolecular potentials depending on a parameter that can be tuned so that the melting line gradually develops a maximum. For each family, the behavior of the function $F(r)$ is studied as the parameter is being tuned, and the reliability of the n-criterion is investigated by comparing its predictions with the results of computer simulation.

We first introduce a family of modified inverse-power (MIP) potentials where the exponent depends on the interparticle distance r in such a way to describe softening of repulsion in a range of distances:

$$u_{\mathrm{MIP}}(r) = \varepsilon(\sigma/r)^{n(r)} \tag{7}$$

with

$$n(r) = n(1 - \alpha e^{-b(1 - r/\sigma)^c}) \tag{8}$$

Here, α is a real number with $0 < \alpha < 1$, b is a positive real number, and c is an even positive integer. The parameter α controls repulsion softening: the greater the value of α, the more significant the softening effect, i.e., the local reduction of $n(r)$. For $\alpha = 0$, the potential in eq 7 has a pure inverse-power functional form, i.e., $u(r) = \varepsilon(\sigma/r)^n$. As α increases, $u_{\mathrm{MIP}}(r)$ becomes, in a range of distances centered around $r = \sigma$, less and less steep, until, for $\alpha = 1$, $u(r)$ has in $r = \sigma$ a horizontal flexus. The parameter b controls the width of the interval where $n(r)$ is significantly smaller than n: the larger the value of b, the smaller this interval. The exponent $n(r)$ attains its smaller value $n_{min} = n(1 - \alpha)$ for $r = \sigma$. In the following, we choose $n = 12$, $c = 2$, and $b = 5$. Figure 1 shows $u_{\mathrm{MIP}}(r)$ and $n(r)$ as a function of r for several values of α.

As α approaches 1, $u_{\mathrm{MIP}}(r)$ develops in a range of r a downward concavity, a feature that is typical of CS potentials. In the region where an interparticle potential $u(r)$ shows a downward, or zero, concavity, i.e., where $u''(r) \leq 0$, the strength of the two-body force $f(r) = -u'(r)$ reduces or at most remains constant as two particles approach each other. Assuming that the repulsion is hardcore-like at small distances and goes to zero sufficiently fast at large distances, such behavior gives origin to two distinct regions where the repulsive force increases as r gets smaller, from which two distinct repulsive length scales emerge: a smaller one ("hard" radius), dominant at the higher pressures, and a larger one ("soft" radius), effective at low pressure. In the range of pressures where the two length scales compete with each other, the system behaves as a "two-state" fluid. A mathematical condition for core softening was proposed by Debenedetti et al.[74] and requires that in some interval $r_1 < r < r_2$, $\Delta[rf(r)] < 0$ for $\Delta r < 0$, together with $u''(r) > 0$ for $r < r_1$ and $r > r_2$. The above conditions are satisfied if, in the interval (r_1, r_2), the product $rf(r)$ (rather than just $f(r)$) reduces with decreasing interparticle separation. This requirement is less rigorous than the condition $u''(r) \leq 0$, and can be met also by a strictly convex potential, yielding a repulsive force that everywhere increases for decreasing r, provided that in a range of interparticle distances the

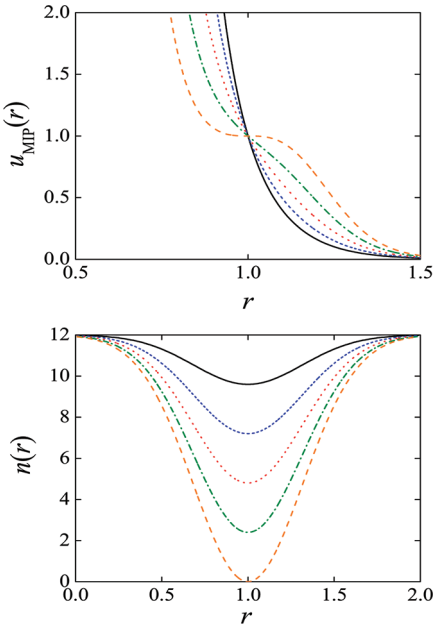

Figure 1. MIP potential (top panel) and the exponent $n(r)$ (bottom panel) for several values of α. $\alpha = 0.2$ (black solid line), 0.4 (blue dashed line), 0.6 (red dotted line), 0.8 (green dash-dotted line), 1 (orange long-dashed line).

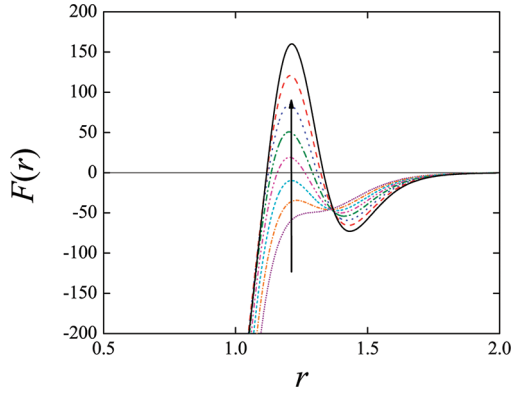

Figure 2. $F(r)$ (ε/σ units) versus r for $u_{MIP}(r)$ for several values of α: $\alpha = 0.35, 0.4, 0.45, 0.5, 0.55, 06, 0.65, 0.7$. The value of α increases in the arrow direction. According to the n-criterion, anomalous melting is possible when $F(r)$ assumes both positive and negative values, i.e., for $\alpha \geq 0.47$.

increasing rate of $f(r)$ is sufficiently small with respect to the adjacent regions.[44] For the MIP potential introduced above, a downward concavity is present for $\alpha \geq 0.72$, and the Debenedetti condition (D-condition) is satisfied for $\alpha \geq 0.68$, while, according to the n-criterion, anomalous melting is possible for $\alpha \geq 0.47$ (Figure 2).

Computer simulation results show that as α increases, the melting line gradually turns from a monotonously increasing behavior to a topology displaying a maximum followed by a re-entrant region (Figure 3). The crossover between the regimes of standard and anomalous melting occurs for α slightly greater than 0.55, both according to SSS and free-energy calculations. This threshold is closer to the estimate of the lower bound of the anomalous region provided by the n-criterion ($\alpha = 0.47$) than to

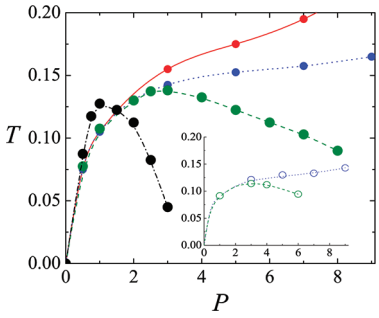

Figure 3. MIP potential. SSS for several values of α (P and T are in reduced units): $\alpha = 0.5$ (red solid line), 0.55 (blue dotted line), 0.6 (green dashed line), 0.8 (black dash-dotted line). Inset: Solid−liquid coexistence points for $\alpha = 0.55$ (blue dotted line), 0.6 (green dashed line), obtained through "exact" free-energy calculations. Lines are guides for the eye.

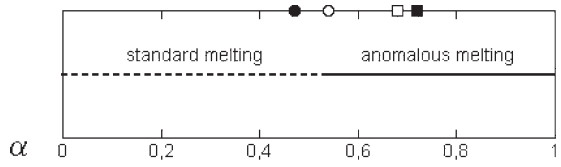

Figure 4. MIP potential. Values of α corresponding to n-criterion (filled circle), onset of anomalous melting according to simulation (open circle), D-condition (open square), and downward concavity rule (filled square).

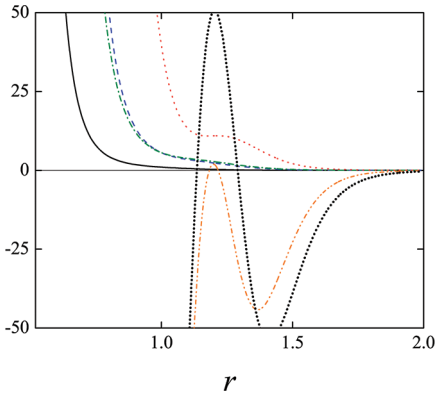

Figure 5. $u_{MIP}(r)$ (black solid line, expressed in ε units), two-body force $f(r) = -u_{MIP}'(r)$ (blue dashed line, ε/σ units), product $rf(r)$ (green dash-dotted line, ε units), second derivative of the potential $u_{MIP}''(r)$ (red dotted line, ε/σ^2 units), third derivative $u_{MIP}''(r)$ (orange long-dashed line, ε/σ^3 units), and $F(r)$ (black thick dotted line, ε/σ units) for $\alpha = 0.55$.

the D-condition ($\alpha = 0.68$) (Figure 4). As shown in Figure 5, the MIP potential for $\alpha = 0.55$ is convex with its first derivative, while a downward concavity is present in its second derivative (that is everywhere positive). For two selected values of α yielding a re-entrant melting curve (i.e., $\alpha = 0.6$ and $\alpha = 0.8$), we calculated the radial distribution function (Figure 6) as well as a number of TDS quantities (Figure 7). For $\alpha = 0.8$, the MIP potential has a region with downward concavity, a feature typical of CS interactions, and thus it is expected to yield two distinct length scales. This is confirmed by the behavior of the radial distribution function $g(r)$ (Figure 6a). In the re-entrant melting pressure range, the heights of the first two peaks change in opposite directions on increasing

pressure, the first peak getting higher and higher and the second one gradually going down. This behavior signals the simultaneous existence of two populations of particles having distinct effective diameters. As pressure increases, the hard inner distance (associated with the first peak) becomes more and more populated at the expenses of the soft larger distance (associated with the second peak), while the position of the two peaks, i.e., the two length scales, remains essentially unaltered. On the contrary, for $\alpha = 0.6$, the behavior of $g(r)$ is radically different. As P increases at constant temperature, the nearest-neighbor peak of $g(r)$ gradually moves toward small r (Figure 6b). Meanwhile, its height first grows, due to increasing proximity with the solid lying at lower temperatures, and then goes down in the pressure range where re-entrant melting occurs. As P increases further, the peak of $g(r)$ grows again, while its position changes less and less sensibly due to the steep small-r repulsion. This behavior is intermediate between that typical of CS fluids (rise and fall of the peak height with pressure signaling ordering−disordering sequence related to the re-entrant region) and that characterinzing standard repulsive interactions such as, say, inverse-power potentials (existence of only one effective length scale that shrinks gradually with pressure). For $\alpha = 0.8$, the system displays, in the fluid phase, density as well as structural and dynamic anomalies, while for $\alpha = 0.6$ the density maximum lays inside the solid region, and the regions of structural and dynamic anomalies, if present, are extremely reduced and lay very close to the melting line maximum, as can be deduced from Figure 7.

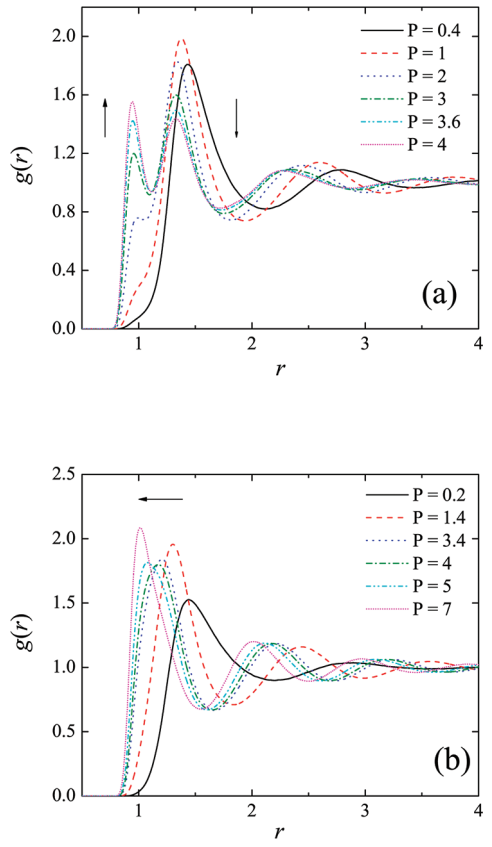

Figure 6. MIP potential. Radial distribution function $g(r)$ for $\alpha = 0.8$ (top panel) and $\alpha = 0.6$ (bottom panel). For $\alpha = 0.8$, lines correspond to $T = 0.2$ and $P = 0.4, 1, 2, 3, 3.6, 4$. For $\alpha = 0.6$, lines correspond to $T = 0.2$ and $P = 0.2, 1.4, 3.4, 4, 5, 7$. The arrows mark the direction of pressure increase.

From the results obtained, the following scenario can be sketched out. As α increases starting from $\alpha = 0$, the MIP potential goes gradually from an inverse-power $1/r^{12}$ form, which is a common representation of the typical excluded-volume interactions resulting from Pauli exclusion principle, to a typical CS form ($\alpha > 0.72$). Around $\alpha = 0.55$, i.e., for a softening of the repulsive interaction much weaker than that leading to a region with downward concavity, a re-entrant portion appears in the melting line. The consequent ordering−disordering transition upon pressure increasing at constant temperature is reflected in the behavior of the peaks of $g(r)$ that, however, shows yet no hint

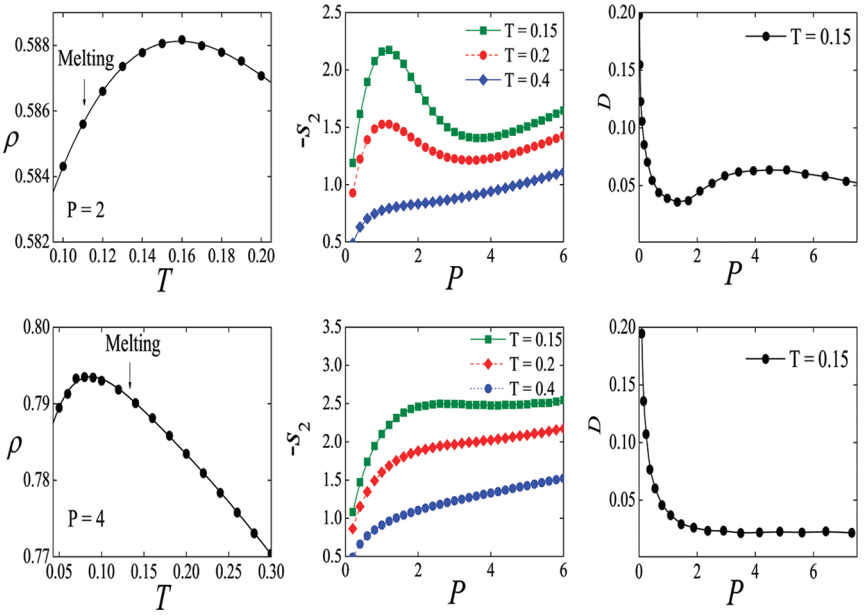

Figure 7. MIP potential. Density ρ versus temperature at constant pressure (reduced units), translational order parameter $-s_2$ (units of k_B) versus pressure at constant temperature, and self-diffusion coefficient D [units of $\sigma(\varepsilon/m)^{1/2}$, where m is particle mass)] versus pressure at constant temperature for $\alpha = 0.8$ (top panel) and $\alpha = 0.6$ (bottom panel).

dx.doi.org/10.1021/jp203939c |J. Phys. Chem. B 2011, 115, 14091–14098

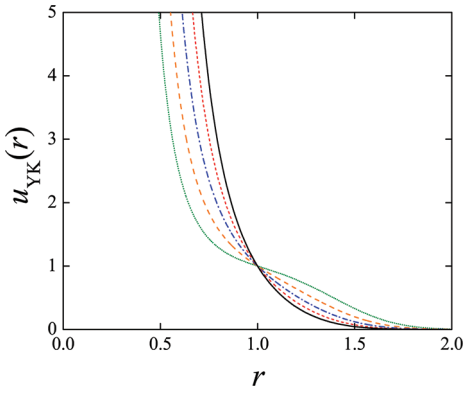

Figure 8. YK potential for different values of the softness parameter a: a = 5 (black solid line), 4 (red dashed line), 3 (blue dash-dotted line), 2 (orange long dashed line), 1 (green dotted line).

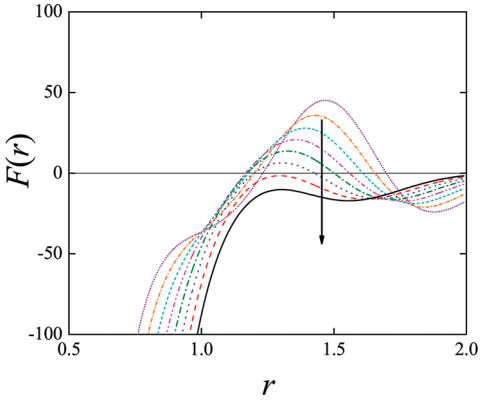

Figure 9. $F(r)$ (ε/σ units) versus r for $u_{YK}(r)$ for several values of a: a = 1, 1.5, 2, 2.5, 3, 3.5, 4, 4.5, 5. The value of a increases in the arrow direction. According to the n-criterion, anomalous melting is possible when $F(r)$ assumes both positive and negative values, i.e., for $a \leq 4.4$.

of the existence of two distinct length scales. TDS anomalies are absent or are restricted to an extremely reduced portion of the PT plane. Only at higher α, where the core-softening condition is satisfied, the two-scale behavior typical of CS systems, is shown by $g(r)$ and TDS anomalies fully develop.

We now consider a model interaction introduced by Yoshida and Kamakura (YK)[75,76]

$$u_{YK}(r) = \varepsilon \exp\left\{a\left(1-\frac{r}{\sigma}\right) - 6\left(1-\frac{r}{\sigma}\right)^2 \ln\left(\frac{r}{\sigma}\right)\right\} \quad (9)$$

with $a > 0$. This potential behaves as r^{-6} for small r, and falls off very rapidly for large r. The softness of the repulsion is controlled by the parameter a: the smaller the value of a, the softer the repulsion (Figure 8). The YK potential has a region with downward curvature for $a \leq 1.9$, the D-condition is met when $a \leq 2.3$, and the n-criterion is satisfied for $a \leq 4.4$ (Figure 9). Note that, since for the YK potential repulsion softness decreases as the parameter a increases, the n-criterion provides an upper bound for the interval of values of a where anomalous melting is possible. According to simulation results (Figure 10), the onset of anomalous melting occurs for a slightly smaller than 4.5, a value that roughly coincides with the estimate of the upper bound of the anomalous region provided by the n-criterion (Figure 11).

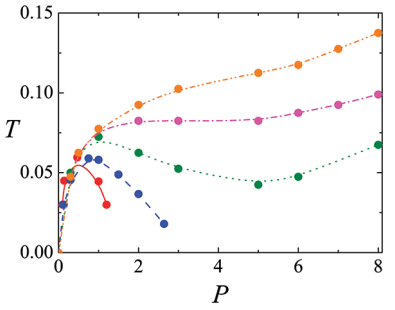

Figure 10. YK potential. SSS for several values of a (P and T are in reduced units): a = 2.1 (red solid line), 3.3 (blue dashed line), 3.9 (green dotted line), 4.5 (magenta dash-dotted line), 5 (orange dash-double dotted line). Lines are guides for the eye.

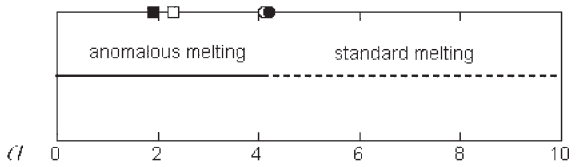

Figure 11. YK potential. Values of a corresponding to downward concavity rule (filled square), D-condition (open square), onset of anomalous melting according to simulation (open circle), and n-criterion (filled circle). The open and the filled circles nearly coincide and partially overlap.

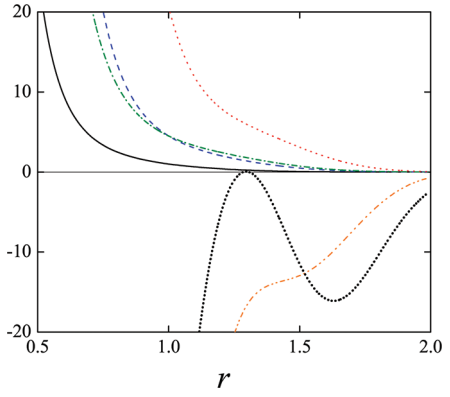

Figure 12. $u_{YK}(r)$ (black solid line, expressed in ε units), two-body force $f(r) = -u_{YK}'(r)$ (blue dashed line, ε/σ units), product $rf(r)$ (green dotted line, ε units), second derivative of the potential $u_{YK}''(r)$ (red dash-dotted line, ε/σ^2 units), third derivative $u_{YK}'''(r)$ (orange long dash-dotted line, ε/σ^3 units), and $F(r)$ (black thick dotted line, ε/σ units) for a = 4.4.

For a = 4.4 the YK potential is convex with its first and second derivative, and only in the third derivative of the potential a downward concave region is to be found (see Figure 12). This is an example of a truly weak softening of the repulsive interaction that nevertheless is sufficient to give origin to anomalous behaviors.

The YK model has been recently investigated through accurate numerical simulation calculations based on free-energy methods. The topology of the melting line, calculated for two selected values of a (a = 2.1 and a = 3.3), is in agreement with that of the SSS. In particular, it was found that for a = 3.3, a value that lays halfway between the D-condition and the n-criterion

dx.doi.org/10.1021/jp203939c |J. Phys. Chem. B 2011, 115, 14091–14098

tresholds, the system exhibits a variety of anomalous behaviors including, in addition to re-entrant melting, a wide spectrum of TDS anomalies and a rich solid polymorphism.[47]

We finally consider the so-called repulsive-step potential, consisting in a hard core plus a finite square shoulder at a larger radius, a system that has been widely investigated in the literature[77] and is able to exhibit re-entrant melting as well as other anomalous behaviors. Since this potential is discontinuous, it is not suited for applying the *n*-criterion. We consider instead a smoothed version of the repulsive-step potential that has been recently introduced:[39]

$$u_{RS}(r) = \varepsilon\left(\frac{\sigma}{r}\right)^{14} + \frac{1}{2}\varepsilon\{1 - \tanh[k_0(r - \sigma_1)]\} \qquad (10)$$

where $k_0 = 10$ and the shoulder width σ_1 is a variable parameter. The *D*-condition is satisfied for $\sigma_1 \geq 1.16\sigma$, while the potential shows a downward concavity for $\sigma_1 \geq 1.17\sigma$. The necessary condition for anomalous melting provided by the *n*-criterion is met for $\sigma_1 \geq 1.05\sigma$. The melting line of this potential was calculated through computer simulation based on free-energy methods for three values of σ_1 (1.15, 1.35, 1.55).[39] Anomalous melting is extremely evident for $\sigma_1 = 1.35\sigma$ and $\sigma_1 = 1.55\sigma$, while for $\sigma_1 = 1.15\sigma$ a nearly flat region is present in the melting line, from which it can be deduced that the onset of re-entrant melting occurs in correspondence with the threshold provided by the *D*-condition.

VI. CONCLUDING REMARKS

In the past decade much efforts have been dedicated to the investigation of simple model systems that, in spite of the isotropic nature of interaction, are able to display anomalous behaviors similar to those observed in substances characterized by much more complex interactions (e.g., water). Particular attention has been focused on trying to determine the class of isotropic intermolecular potentials able to generate anomalous behaviors. Up to not long ago, it was generally assumed that the presence of a region with downward or zero concavity in the repulsive component of the potential, and the consequent existence of two distinct repulsive length scales, was a requisite for anomalous behaviors.[43,78] Recently, it has been shown that such behaviors may occur also in systems with strictly convex repulsive potentials where repulsion softening is so weak that the two-scale "paradigm" holds no more.[47]

The analysis presented in this paper aims to extend our comprehension of the features that an isotropic intermolecular potential should possess in order to yield anomalous behaviors. We derive a single-phase criterion that provides a necessary condition, expressed in terms of the first three derivatives of the interparticle potential, for the occurrence of anomalous melting. This criterion has been tested against numerical simulation for a number of radially symmetric models. The "distance" between the necessary condition threshold and the onset of anomalous melting (as estimated through simulation) depends on the system considered. In some cases, the two boundaries approximately coincide, while in others they are less close. Our results show that, in general, the onset of anomalous melting occurs in a region that is bounded on one end by the necessary condition threshold and on the other end by the Debenedetti core softening condition. This finding, in agreement with some recent results,[47] show that the class of isotropic systems able to yield anomalous behaviors is much wider than commonly assumed. In the case of the MIP potential, we investigate in detail how the system behavior changes when the repulsion is gradually softened and goes from the inverse-power form to that typical of CS potentials. The first anomalous behavior to become evident is re-entrant melting, while TDS anomalies are located in the metastable fluid region or are confined to a vanishingly small portion of the stable fluid phase. At this stage, the $g(r)$, although reflecting the ordering−disordering transition related to re-entrant melting, does not show the two-scale features typical of CS systems. Only when repulsion softening is more significant and the core-softening condition is satisfied, the two-scale behavior is exhibited by the $g(r)$, and the regions of TDS anomalies extend over significant domains of the PT plane.

AUTHOR INFORMATION

Corresponding Author

*E-mail: malescio@unime.it.

Notes

[§]E-mail: saija@me.cnr.it.

REFERENCES

(1) Young, D. A. *Phase Diagrams of the Elements*; University of California: Berkeley, CA, 1991.
(2) Debenedetti, P. G. *Metastable Liquids*; Princeton University Press: Princeton, NJ, 1996.
(3) Buldyrev, S. V.; Malescio, G.; Angell, C. A.; Giovambattista, N.; Prestipino, S.; Saija, F.; Stanley, H. E.; Xu, L. *J. Phys.: Condens. Matter* **2009**, *21*, 504106.
(4) Mishima, O.; Stanley, H. E. *Nature* **396**, *1998*, 329.
(5) Sastry, S.; Angell, C. A. *Nat. Mater.* **2003**, *2*, 739.
(6) Katayama, Y.; Mizutani, T.; Utsumi, W.; Shimomura, O.; Yamakata, M.; Kunakoshi, K. *Nature* **2000**, *403*, 170.
(7) Meade, C.; Hemley, R. J.; Mao, H. K. *Phys. Rev. Lett.* **1992**, *69*, 1387.
(8) Thurn, H.; Ruska, J. *J. Non-Cryst. Solids* **1976**, *22*, 331.
(9) Bundy, F. P. *Phys. Rev.* **1959**, *115*, 274.
(10) Rapoport, E. *J. Chem. Phys.* **1967**, *46*, 2891.
(11) Jayaraman, A.; Newton, R. C.; McDonough, J. M. *Phys. Rev.* **1967**, *159*, 527.
(12) Errandonea, D.; Schwager, B.; Ditz, R.; Gessmann, C.; Boehler, R.; Ross, M. *Phys. Rev. B* **2001**, *63*, 132104.
(13) Hanfland, M.; Syassen, K.; Christensen, N. E.; Novikov, D. L. *Nature* **2000**, *408*, 174.
(14) McMahon, M. I.; Gregoryanz, E.; Lundegaard, L. F.; Loa, I.; Guillaume, C.; Nelmes, R. J.; Kleppe, A. K.; Amboage, M.; Wilhelm, H.; Jephcoat, A. P. *Proc. Natl. Acad. Sci. U.S.A.* **2007**, *104*, 17297.
(15) Mukherjee, G. D.; Boehler, R. *Phys. Rev. Lett.* **2007**, *99*, 225701.
(16) Eremets, M. I.; Trojan, I. A. *JETP Lett.* **2009**, *89*, 174.
(17) Eggert, J. H.; Hicks, D. G.; Celliers, P. M.; Bradley, D. K.; McWilliamson, R. S.; Jeanloz, R.; Miller, J. E.; Boehly, T. R.; Collins, G. W. *Nat. Phys.* **2010**, *6*, 40.
(18) Pfaffenzeller, O.; Hohl, D. *J. Phys.: Condens. Matter* **1997**, *9*, 11023.
(19) Scandolo, S. *Proc. Natl. Acad. Sci. U.S.A.* **2003**, *100*, 3051.
(20) Bonev, S. A.; Schwegler, E.; Ogitsu, T.; Galli, G. *Nature* **2004**, *431*, 431.
(21) Boates, B.; Bonev, S. A. *Phys. Rev. Lett.* **2009**, *102*, 015701.
(22) Raty, J. Y.; Schwegler, E.; Bonev, S. A. *Nature* **2007**, *449*, 448.
(23) Tamblyn, I.; Raty, J. Y.; Bonev, S. A. *Phys. Rev. Lett.* **2008**, *101*, 075703.
(24) Correa, A. A.; Bonev, S. A.; Galli, G. *Proc. Natl. Acad. Sci. U.S.A.* **2006**, *103*, 1204.
(25) Hemmer, P. C.; Stell, G. *Phys. Rev. Lett.* **1970**, *24*, 1284.
(26) Sadr-Lahijany, M. R.; Scala, A.; Buldyrev, S. V.; Staley, H. E. *Phys. Rev. Lett.* **1998**, *81*, 4895.
(27) Jagla, E. A. *Phys. Rev. E* **1998**, *58*, 1478.

(28) Watzlawek, M.; Likos, C. N.; LÖwen, H. *Phys. Rev. Lett.* **1999**, *82*, 5289.
(29) Franzese, G.; Malescio, G.; Skibinsky, A.; Buldyrev, S. V.; Stanley, H. E. *Nature* **2001**, *409*, 692.
(30) Franzese, G.; Malescio, G.; Skibinsky, A.; Buldyrev, S. V.; Stanley, H. E. *Phys. Rev. E* **2002**, *66*, 051206.
(31) Malescio, G.; Franzese, G.; Pellicane, G.; Skibinsky, A.; Buldyrev, S. V.; Stanley, H. H. *J. Phys.: Condens. Matter* **2002**, *14*, 2193.
(32) Malescio, G.; Pellicane, G. *Nat. Mater.* **2003**, *2*, 97.
(33) Skibinsky, A.; Buldyrev, S. V.; Franzese, G.; Malescio, G.; Stanley, H. E. *Phys. Rev. E* **2004**, *69*, 061206.
(34) Malescio, G.; Pellicane, G. *Phys. Rev. E* **2004**, *70*, 021202.
(35) Malescio, G.; Franzese, G.; Skibinsky, A.; Buldyrev, S. V.; Stanley, H. H. *Phys. Rev. E* **2005**, *71*, 061504.
(36) Yan, Z.; Buldyrev, S. V.; Giovambattista, N.; Stanley, H. E. *Phys. Rev. Lett.* **2005**, *95*, 130604.
(37) Gibson, H. M.; Wilding, N. B. *Phys. Rev. E* **2006**, *73*, 061507.
(38) Malescio, G. *J. Phys.: Condens. Matter* **2007**, *19*, 073101.
(39) Fomin, Y. D.; Gribova, N. V.; Ryzhov, V. N.; Stishov, S. M.; Frenkel, D. *J. Chem. Phys.* **2008**, *129*, 064512.
(40) Fomin, Y. D.; Tsiok, E. N.; Ryzhov, V. N. *J. Chem. Phys.* **2011**, *134*, 044523.
(41) Pauschenwein, G. J.; Kahl, G. *Soft Matter* **2008**, *4*, 1396.
(42) Malescio, G.; Saija, F.; Prestipino, S. *J. Chem. Phys.* **2008**, *129*, 241101.
(43) de Oliveira, A. B.; Netz, P. A.; Barbosa, M. *Europhys. Lett.* **2009**, *85*, 36001.
(44) Saija, F.; Prestipino, S.; Malescio, G. *Phys. Rev. E* **2009**, *80*, 031502.
(45) Vilaseca, P.; Franzese, G. *J. Chem. Phys.* **2010**, *133*, 084507.
(46) Lascaris, E.; Malescio, G.; Buldyrev, S. V.; Stanley, H. E. *Phys. Rev. E* **2010**, *81*, 031201.
(47) Prestipino, S.; Saija, F.; Malescio, G. *J. Chem. Phys.* **2010**, *133*, 144504.
(48) Bosio, L.; Chen, S. H.; Teixeira, J. *Phys. Rev. A* **1983**, *27*, 1468.
(49) Sciortino, F.; Geiger, A.; Stanley, H. E. *Phys. Rev. Lett.* **1990**, *65*, 3452.
(50) Sciortino, F.; Geiger, A.; Stanley, H. E. *Nature* **1991**, *354*, 218.
(51) Canpolat, M.; Starr, F. W.; Scala, A.; Sadr-Lahijany, M. R.; Mishima, O.; Havlin, S.; Stanley, H. E. *Chem. Phys. Lett.* **1998**, *294*, 9.
(52) Schwegler, E.; Galli, G.; Gygi, F. *Phys. Rev. Lett.* **2000**, *84*, 2429.
(53) Soper, A. K.; Ricci, M. A. *Phys. Rev. Lett.* **2000**, *84*, 2881.
(54) Botti, A.; Bruni, F.; Isopo, A.; Ricci, M. A.; Soper, A. K. *J. Chem. Phys.* **2002**, *117*, 6196.
(55) Yamada, M.; Mossa, S.; Stanley, H. E.; Sciortino, F. *Phys. Rev. Lett.* **2002**, *88*, 195701.
(56) Saitta, A. M.; Datchi, F. *Phys. Rev. E* **2003**, *67*, 020201R.
(57) Paschek, D. *Phys. Rev. Lett.* **2005**, *94*, 217802.
(58) Strassle, T.; Saitta, A. M.; Le Godec, Y.; Hamel, G.; Klotz, S.; Loveday, J. S.; Nelmes, R. J. *Phys. Rev. Lett.* **2006**, *96*, 067801.
(59) Errington, J. R.; Debenedetti, P. G. *Nature* **2001**, *409*, 318.
(60) Esposito, R.; Saija, F.; Saitta, A. M.; Giaquinta, P. V. *Phys. Rev. E* **2006**, *73*, 040502(R).
(61) Mallamace, F.; Broccio, M.; Corsaro, C.; Faraone, A.; Majolino, D.; Venuti, V.; Liu, L.; Mou, C. Y.; Chen, S. H. *Proc. Natl. Acad. Sci. U.S.A.* **2007**, *104*, 424.
(62) Yan, Z.; Buldyrev, S. V.; Kumar, P.; Giovambattista, N.; Stanley, H. E. *Phys. Rev. E* **2008**, *77*, 042201.
(63) Xu, L.; Mallamace, F.; Yan, Z.; Starr, F. W.; Buldyrev, S. V.; Stanley, H. E. *Nat. Phys.* **2009**, *5*, 565.
(64) Tanaka, H.; Kurita, R.; Mataki, M. *Phys. Rev. Lett.* **2004**, *92*, 025701.
(65) Kurita, R.; Tanaka, H. *Science* **2004**, *306*, 845.
(66) Saija, F.; Prestipino, S.; Malescio, G. *Phys. Chem. Liq.* **2010**, *48*, 477.
(67) McMillan, P. F. *J. Mater. Chem.* **2004**, *14*, 1506.
(68) Lindemann, F. A. *Z. Phys.* **1910**, *11*, 609.
(69) Lennard-Jones, J. E.; Devonshire, A. F. *Proc. R. Soc. London A* **1037**, *163*, 53. **1938**, *165*, 1.
(70) Kirkwood, J. G. *J. Chem. Phys.* **1950**, *18*, 380.
(71) Yoshida, T.; Kamakura, S. *Prog. Theor. Phys.* **1974**, *52*, 822.
(72) Prestipino, S.; Saija, F.; Malescio, G. *Soft Matter* **2009**, *5*, 2795.
(73) Malescio, G.; Prestipino, S.; Saija, F. *Mol. Phys.* **2011**, DOI: 10.1080/00268976.2011.609146.
(74) Debenedetti, P. G.; Raghavan, V. S.; Borick, S. S. *J. Phys. Chem.* **1991**, *95*, 4540.
(75) Yoshida, T.; Kamakura, S. *Prog. Theor. Phys.* **1972**, *47*, 1801.
(76) Kamakura, S.; Yoshida, T. *Prog. Theor. Phys.* **1972**, *48*, 2110.
(77) Young, D. A.; Alder, B. J. *Phys. Rev. Lett.* **1977**, *38*, 1213.
(78) Vilaseca, P.; Franzese, G. *J. Non-Cryst. Solids* **2011**, *357*, 419.